March – April 2020
ISSN: 0193-4120 Page No. 23306 – 23314

The Influence of Addition Quaternary Ammonium Chloride to Prevent CO_2 Corrosion on ASTM A106 Grade B Steel

[1]Lamria Mora Dhea Friskila, [2]Dr. Ir. Rini Riastuti, [3]Muhammad Asep Yudistira

[1,2,3]Universitas Indonesia, Faculty of Engineering, Metallurgy and Materials Engineering,
Jl. Kampus Baru UI, Depok, East Java, Indonesia

Article Info
Volume 83
Page Number: 23306 – 23314
Publication Issue:
March - April 2020

Article History
Article Received*: 24 July 2019*
Revised*: 12 September 2019*
Accepted*: 15 February 2020*
Publication*: 30 April 2020*

Abstract

This study investigated Octadecyl Trimethyl Ammonium Chloride (OTAC) as a corrosion inhibitor for ASTM A106 Grade B steel in 3.0 wt% NaCl purged with 1 bar CO2. Temperature variation of 40°C and 90°C and inhibitor different concentrations were applied. The examination engaged potentiodynamic polarization technique. The data obtained became references in determining the adsorption isotherm type. Surface characterization exploiting a Scanning Electron Microscope (SEM) and an Energi Dispersive X-Ray Spectroscopy (EDS) helped discover the inhibition mechanism. Several results gained are as follows. First, the more the temperature increases, the more efficient the inhibitor is. Secondly, the inhibitor follows Langmuir's adsorption isotherm while the value of adsorption surface energy (ΔG) indicates the adsorption mechanism takes place both chemically and physically. Last, the SEM-EDS analysis results in a large decline in oxygen, a main factor of sweet corrosion.

Keywords; *Adsorption, Inhibitor, Sweet Corrosion, Quaternary Ammonium Chloride.*

I. INTRODUCTION

Mild steel is commonly used in various industries because of its fair properties and affordable price. However, the corrosion resistance of this steel is only in an average level [1-2] while corrosion is very undesirable. Morevoer, in the oil and gas industry, there are adverse conditions where CO^2 exists during exploration from wells. This CO^2 existence leds to a very detrimental corrosion, sweet corrosion [3-5]. This corrosion is so dangerous due to its unpredictable corrosion rate and development [6]. To overcome this, a preventive step in the form of inhibitor is taken.

As an inhibitor, quaternary ammonium compounds are comprised of cationic surfactant groups, namely surfactants which have a positive charge on the hydrophobic interface group [7]. These cationic surfactant groups have proven effective to protect metal surfaces [8-11]. Other than that, the quaternary ammonium compound consists of a long alkyl group. A previous study concluded that the longer the alkyl group, the lower the effectiveness since there will be less cationic surfactants able to react [12]. Another finding is that adding temperature raises the performance of inhibitor. Nevertheless, there is no description of injecting CO^2 gas.

March – April 2020
ISSN: 0193-4120 Page No. 23306 – 23314

This study aims at discovering the effectiveness of quaternary ammonium-based inhibitor at various temperatures with the presence of CO^2. The investigation was based on the results of linear polarization and involved the surface adsorption and appearance analysis.

II. Material And Methods

A. Material and Inhibitor.

The investigation was carried out on an ASTM A106 Grade B steel, the composition of which is shown in Table 1.

Table I
Chemical composition of ASTM A106 Grade B steel (wt%).

C	Si	Mn	P	S	Cr	Mo
0.14	0.23	0.81	0.004	0.002	0.06	0.01
Ni	**Cu**	**V**	**Nb**	**Ti**	**B**	
0.05	0.05	0.002	0.01	0.002	0.0001	

The inhibitor, ammonium quaternery salt compounds, contains cationic surfactant groups having a positive charge on the hydrophobic interface group. This compound has the general formula. of R4N + X, where R is one or more alkyl or heterocyclic groups with long chains while X is a halide anion, such as chloride and bromide [8].

The inhibitor, Octadecyl Trimethyl Ammonium Chloride (OTAC), was mixed with 3.0 wt% NaCl. The test solution concentration varies from 25 ppm to 50 ppm and 75 ppm.

B. Electrodes Preparation.

Before the potentiodynamic exploration was conducted, the ASTM A106 Grade B steel was prepared to be a working electrode. The ASTM A106 Grade B steel pipe was cut and grinded into a cylinder with a diameter of 10 mm and a surface area of 15.87 cm^{-1}. Next, the sample was soldered with Cu wire as a connector, mounted with epoxy resin, and then left for 12 hours until it hardened. Afterwards, it was rubbed with a 80 to 300 grid sandpaper and 10% acetone-washed.

C. Potentiodynamic Measurements.

This test was conducted through a Gamry Potentiostat/Galvanostat instrument and controlled by a Gamry Echem Analyst 6.30 software package. The electrodes used included a Saturated Calomel Electrode (SCE) as a reference electrode, a platinum electrode as a counter electrode, and several samples that had been prepared as working electrodes. The test was done at 40°C and 90°C with 1 bar CO_2 gas purging during the process. The initial potential and the final potential were set at -0,250 V and 0,250 V to the open circuit voltage.

The results of the above investigations became quantitative parameters to interpretate the inhibitor adsorption capability. They are anodic tafel slope (βa), cathodic tafel slope (βc), Icorr, Ecorr, and corrosion rate.

D. Surface Characterization.

After the electrochemical experiments, the mild steel specimens were stored in desiccators to undergo the surface morphological investigation. The micrographs were taken using SEM operated at an accelerating voltage of 20 kV. The EDS system in the microscope was applied to project the composition of the elements on the surface. Both SEM and EDS

March – April 2020
ISSN: 0193-4120 Page No. 23306 – 23314

characterizations were done using an Inspect F50 scanning electron microscope from Field Electron and Ion Company equipped with an EDS analyzer.

III. Results And Discussions

A. Fourier Transform Infrared Spectroscopy (FTIR).

The FTIR analysis helped verify the functional groups contained in the inhibitor. Through this exploration, a spectrum would be presented as a reference in determining the available functional groups. The results of FTIR study on OTAC are shown in Fig. 1.

OTAC is a type of quaternary ammonium compound with a very long C chain. OTAC has a molecule formula of $C_{21}H_{46}NCl$. The FTIR examination produced several main spectrums that proved the chemical chain in this inhibitor. They are 1072 cm^{-1} for the asymmetric and symmetric stretching N + -C, and 2854 and 2924 cm^{-1} for CH3 [13]. This implies that OTAC consists of two main functional groups making it a compound with C18H37 - N^{+} $(CH_3)_3Cl^{-}$.

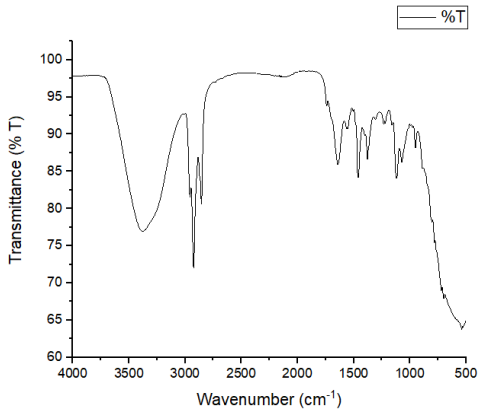

Figure 1. FTIR test result of OTAC.

B. Potentiodynamic Test.

Potentiodynamic behavior of OTAC has been investigated based on Tafel extrapolation. The anodic/cathodic polarization curves for OTAC at different temperatures are shown in Fig. 2. Based on the graph, the addition of inhibitor at various concentrations results in a similar Tafel curve. This indicates that the inhibition mechanism of OTAC is the same as that on the A103 Grade B steel surface. Based on the data in Table 1, the addition of OTAC shifts the E_{corr} and I_{corr} values as well as the slope of β_a and β_c. A shift in E_{corr} value of more than 85 mV is categorized as an anodic or cathodic inhibitor [14]. Meanwhile, the shifts in E_{corr} values at temperatures of 40°C and 90°C are 175 mV and 77 mV, respectively to blank. This signals that OTAC acted as an either anodic or cathodic inhibitor at 40°C, but as both anodic and cathodic inhibitor at 90°C. The evident is shown in Table 2. The data expose that there is a significant shift in the slope βc value at 40°C. However, this case does not happen at 90°C. This implies that OTAC acted as a cathodic inhibitor at 40°C.

Based on the data from Tafel extrapolation, the polarization resistance values can be calculated based on Eq. 1, becoming a reference in the effectiveness of inhibitor.

$$Rp = \frac{\beta a \times \beta c}{2.3 icorr\ (\beta a + \beta c)} \qquad (1)$$

March – April 2020
ISSN: 0193-4120 Page No. 23306 – 23314

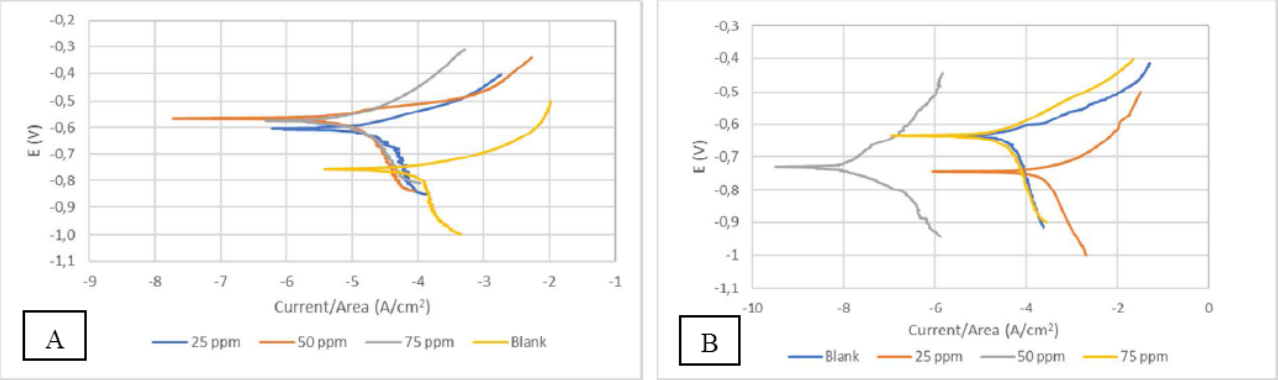

Figure 2. Potentiodynamic polarization curves for the ASTM A106 Grade B steel in 3.0 wt% NaCl in the absence and presence of different concentrations of OTAC at (A) 40°C and (B) 90°C.

The polarization resistance values and inhibitor efficiency are in Table 2. The addition of OTAC at various concentrations resulted in a decrease in Icorr and an increase in the value of Rp at a concentration of 50 ppm, then a decrease in 75 ppm. This happened in both temperature conditions. This implies that OTAC performs optimally at 50 ppm. It indicates that the addition of 75 ppm was so dense that the C chain appeared in the solution. Thus, the cationic surfactant in OTAC could not function optimally.

The effect of temperature addition on OTAC shows that the higher the temperature is, the better the OTAC works. The heat movement of organic molecules is accelerating and the adsorption capacity of the inhibitor on metal surface is strengthening due to higher temperatures [12]. This is shown by the value of Rp in the addition of 50 ppm OTAC at a temperature of 90°C in which a significant jump in the value of Rp happened.

Table II

Potentiodynamic polarization parameters for the ASTM A106 Grade B steel in 3.0 wt% NaCl in the absence and presence different concentration of OTAC.

Temperature [°C]	Inhibitor Dose [ppm]	I_{corr} [A.cm^{-2}]	E_{corr} vs SCE [V]	ßa [V.dec^{-1}]	ßc [V.dec^{-1}]	R_p [ohm]	Inhibitor Efficiency [%]
40	Blank	0,3 x 10^{-3}	-0,757	0,141	2,77 x 10^{7}	2,04 x 10^{2}	
	25	3,5 x 10^{-5}	-0,603	0,1153	5,94 x 10^{-1}	1,20 x 10^{3}	82,9
	50	6,67 x 10^{-6}	-0,568	0,0724	2,51 x 10^{-1}	3,66 x 10^{3}	94,4
	75	2,54 x 10^{-4}	-0,573	0,1964	5,97 x 10^{-1}	2,53 x x 10^{3}	91,9
90	Blank	6,67 x 10^{-4}	-0,743	0,1288	1,08	7,50 x 10^{1}	
	25	6,85 x 10^{-5}	-0,635	0,0698	6,08 x 10^{-1}	3,97 x 10^{2}	81,1
	50	2,56 x 10^{-8}	-0,728	0,1481	2,0 x 10^{-1}	1,13 x 10^{6}	99,9
	75	3,52 x 10^{-5}	-0,634	0,0795	3,30 x 10^{-1}	7,91 x 10^{2}	90,5

C. Adsorption Isotherm.

The mechanism of adsorption can be determined by finding the adsorption mode of the inhibitor. One

March – April 2020
ISSN: 0193-4120 Page No. 23306 – 23314

method to determine the adsorption mode is to look at the adsorption isotherm of the inhibitor. The adsorption process of an inhibitor can be explored thermodynamically at a spesific temperature from the relationship between surface coverage and the concentration of the inhibitor addition [15]. So far, the Langmuir mechanism is the best of the others. To prove this, a plot between M vs M/θ was carried out as displayed in Fig. 3.

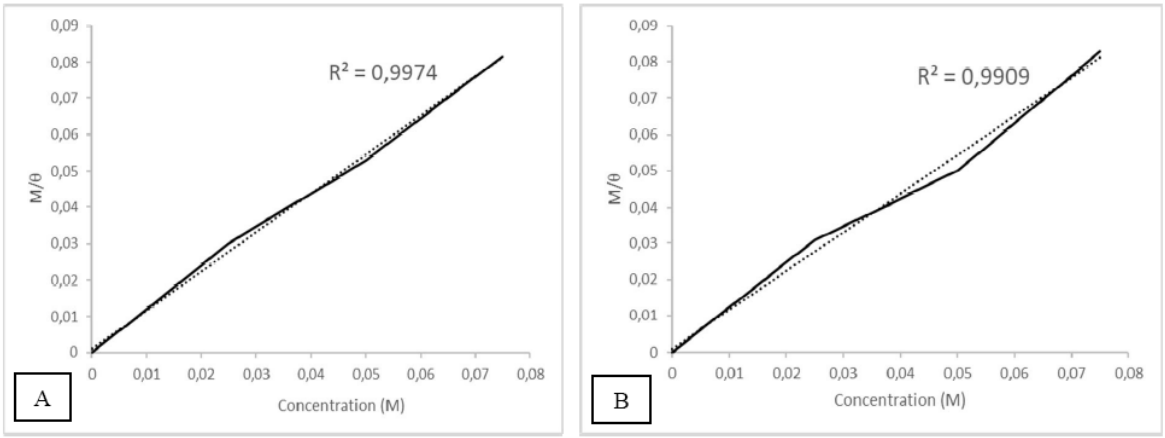

Figure 3. Langmuir's adsorption isotherm model on the ASTM A106 Grade B steel surface of prepared OTAC in 3.0 wt% NaCl solution at (A) 40°C and (B) 90°C.

According to the two graphs, Langmuir fits at both temperatures, suggesting that the inhibition is monolayer. This type of isotherm was evaluated based on Eq. 2 below.

$$\frac{Cinh}{\theta} = \frac{1}{Kads} + Cinh \qquad (2)$$

The above Eq. shows that K_{ads} the adsorptive equilibrium constant, C is the concentration of inhibitor, and θ is the surface coverage. The value of surface coverage is the same as that of inhibitor efficiency. This equation helped discover the value of K_{ads} and determine the value of surface energy (G) based on Eq. 3 with the 8.314 $J.mol^{-1}.K^{-1}$ value of R.

$$K = \frac{1}{55,5}\exp\left(\frac{-\Delta G°ads}{RT}\right) \qquad (3)$$

The value of 55.5 is the molar concentration of water in solution in units ($mol.L^{-1}$). A negative ΔG_{ads} value along with a large K value signals a spontaneous adsorption process and good chemical stability from the inhibitor compound obtained from the chemical bond between the metal and the inhibitor molecule.

The adsorption process will occur if ΔGads is negative, indicating that the reaction happens spontaneously [16]. A value of ΔGads inhibitor less than –40 $kJ.mol^{-1}$ implies that the inhibitor is included in chemisorption. On the other hand, the inhibitor will be included in physical adsorption if the value of ΔGads inhibitor is more than -20 $kJ.mol^{-1}$ [17]. Morover, if the value of ΔGads is between -40

March – April 2020
ISSN: 0193-4120 Page No. 23306 – 23314

kJ.mol^{-1} and -20 kJ.mol^{-1}, the adsorption process will occur through both chemisorption and physisorption [18]. Based on Eq. 2 and 3, the values of Kads and ΔGads are 338.61 and -25.6 kJ.mol^{-1}, respectively. It implies that OTAC inhibits metal surfaces through both chemisorption and physisorption.

D. Scanning Electron Microscopy (SEM).

Knowing the surface condition of ASTM A106 grade B steel after electrochemical investigation involved SEM-EDS characterization. This test was conducted at the optimal inhibitor concentration, 50 ppm, at each temperature. Then the results were compared with those without inhibitor.

As seen in Fig. 4, there is a similar phenomenon. In terms of EDS (the bottom part of the picture), a decrease in the value of C and O exists in the sample with the inhibitor addition. The existence of C and O atoms formed the atom of sweet corrosion products, $FeCO_3$. The decrease in the value of these two atoms signals the restrained corrosion process. At a temperature of 40°C, the decrease in the amount of O reached 32.22% and that of C hit 14.9 % of the total area. Meanwhile, at a temperature of 90°C, the number of O atoms decreased sharply, about 60% of the total percent area.

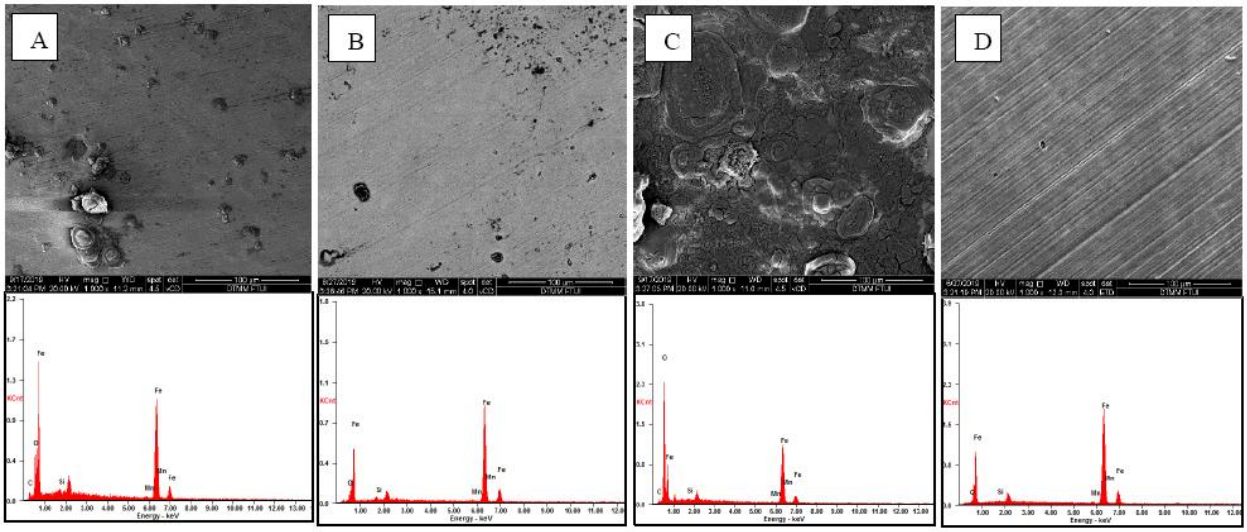

Figure 4. The SEM (upper) and EDS (below) test result of ASTM A106 Grade B steel surface after electrochemical testing at (A) 40°C with no inhibitor, (B) 40°C with 50 ppm of OTAC, (C) 90°C with no inhibitor, and (D) 90°C with 50 ppm of OTAC.

Meanwhile, from the SEM perspective, in the blank condition, both temperatures show non-uniform surface condition. This implies pitting corrosion. At 90°C, Fig. 4 (C), the surface uniformity is much higher than that at 40°C, Fig. 4 (A). Bad surface conditions happened at high temperatures in a CO_2 environment. After adding the same amount of inhibitor, their surface uniformity increased.

March – April 2020
ISSN: 0193-4120 Page No. 23306 – 23314

However, a significant change occurred at 90°C. In Fig. 4 (D), the surface condition is much smoother than that in Fig 4 (B). Thus, it can be concluded the results of surface characterization reinforces the statement in the previous discussion, that OTAC functions optimally at high temperatures.

E. Adsorption Mechanism.

As previously stated, OTAC inhibition behavior can take place both chemically and physically. Physically, OTAC directly bound to metal surfaces following the van der walls force. In addition, the OTAC main hydrophilic part of —$^{+}N(CH_3)_3$ attacked the C-steel surface while that of (–C_6H_{33}) extended to the solution face. Furthermore, OTAC protected the steel surface through chemical adsorption process. In chloric solution, the surface of mild steel would be positively charged. This occured based on the anodic dissolution mechanism of mild steel shown by Eq. 4–7.

$$Fe + Cl^- \rightarrow (FeCl^-)_{ads} \quad (4)$$

$$(FeCl^-)_{ads} \leftrightarrow (FeCl)_{ads} + e^- \quad (5)$$

$$(FeCl)_{ads} \rightarrow (FeCl^+) + e^- \quad (6)$$

$$(FeCl^+) \leftrightarrow Fe^{+2} + Cl \quad (7)$$

This fact made protonated molecules ($^{+}N(CH_3)_3$) difficult to bind to a positive metal surface. Since chloride ions had a smaller degree of hydration and thus they brought excess negative charges in the vicinity of the interface and supported more adsorption of the positively charged inhibitor molecules, the protonated compounds adsorbed through electrostatic interactions between the positively charged molecules and the negatively charged metal surface. Another possible scheme is that the chloride ion in OTAC acted as a mediator between the protonated molecule and the metal surface. Chloride ion was negatively charged and as a result, the specific adsorption of chloride ion occured onto mild steel surfaces, bringing about negatively charged surfaces of steel. Chloride ion acted like a sandwich film barrier.

IV. Conclusion

In view of the results of all investigations over, several conclusions are drawn as follows. First, OTAC functions effectively in NaCl solution and a CO_2 environment. Secondly, 50 ppm is the optimum concentration of the addition of OTAC in which OTAC effectively works. Thirdly, in the process of decreasing its corrosion, OTAC fulfills the Langmuir isotherm adsorption model with a spontaneous reaction. Last, the effectiveness of OTAC is evident from the results of surface characterization, where the SEM-EDS analysis shows a reduction in the amount of oxygen, the existence of pitting corrosion, and a smoother surface appearance.

V. Acknowledgement

This work was subsidized by the Dana Hibah PITTA B 2019 - University of Indonesia under grant number: NKB-0778/UN2.R3.1/HKP.05.00/2019

VI. References

[1] Lgaz, H., Chung, I.-M., Albayati, M. R., Chaouiki, A., Salghi, R., and Mohamed, S. K. “Improved Corrosion Resistance of Mild Steel in Acidic Solution by Hydrazone Derivatives: An Experimental and

March – April 2020
ISSN: 0193-4120 Page No. 23306 – 23314

Computational Study," Arabian Journal of Chemistry, August 2018.

[2] Singh, M., "A green Approach: A corrosion inhibition of mild steel by adhatoda vasica plant extract in 0.5 M H2SO4." Journal of Materials and Environmental Science, vol. 4, pp 117-126, Januari 2013.

[3] Perez, T.E., "Corrosion in the Oil and Gas Industry: An Increasing Challenge for Materials," JOM, vol. 65, pp. 1033-1042, August 2013.

[4] Kahyarian, A., Singer, M., Nesic, S., "Modeling of uniform CO2 corrosion of mild steel in gas transportation systems: a review." J. Nat. Gas Sci. Eng., vol. 29, pp. 530–549, February 2016.

[5] M.B. Kermani and A. Morshed, "Carbon Dioxide Corrosion in Oil and Gas Production," A Compendium, Corrosion, vol. 59 pp. 659, August 2003.

[6] Schlumberger, "Corrosion-the longest war," Oilfield Review, no. 2, May 2016.

[7] Fu, E., McCue, K., and Boesenberg, D., "Chemical Disinfection of Hard Surfaces – Household, Industrial and Institutional Settings," Handbook for Cleaning/Decontamination of Surfaces, pp. 573–592, December 2007.

[8] Zhang, J., Song, W. W., Shi, D. L., Niu, L. W., Li, C. J., and Du, M, "A dissymmetric bis-quaternary ammonium salt gemini surfactant as effective inhibitor for Q235 steel in hydrochloric acid," Progress in Organic Coatings, vol. 75, no. 4, pp. 284–291, August 2012.

[9] Fei, F., Hu, J., Wei, J., Yu, Q., and Chen, Z., "Corrosion performance of steel reinforcement in simulated concrete pore solutions in the presence of imidazoline quaternary ammonium salt corrosion inhibitor," Construction and Building Materials, vol. 70, pp. 43–53, November 2014.

[10] Abd-Elaal, A. A., Shaban, S. M., and Tawfik, S. M., "Three Gemini cationic surfactants based on polyethylene glycol as effective corrosion inhibitor for mild steel in acidic environment," Journal of the Association of Arab Universities for Basic and Applied Sciences, vol. 24(1), pp. 54–65, March 2017.

[11] Migahed, M. A., elgendy, A., EL-Rabiei, M. M., Nady, H., and Zaki, E. G., " Novel Gemini cationic surfactants as anti-corrosion for X-65 steel dissolution in oilfield produced water under sweet conditions: Combined experimental and computational investigations," Journal of Molecular Structure,vol. 1159, pp. 10–22.May 2018

[12] Gao, M., Zhang, J., Liu, Q., Li, J., Zhang, R., and Chen, G., "Effect of the alkyl chain of quaternary ammonium cationic surfactants on corrosion inhibition in hydrochloric acid solution," Comptes Rendus Chimie., vol. 22, no. 5, pp. 355-362, May 2019.

[13] Migahed, M. A., Shaban, M. M., Fadda, A. A., Ali, T. A., and Negm, N. A., "Synthesis of some quaternary ammonium gemini surfactants

March – April 2020
ISSN: 0193-4120 Page No. 23306 – 23314

and evaluation of their performance as corrosion inhibitors for carbon steel in oil well formation water containing sulfide ions," RSC Advances, vol. 5, no. 126, pp. 104480–104492, November 2015.

[14] A. A. Al-Amiery, F. A. B. Kassim, A. A. H. Kadhum, and A. B. Mohamad, "Synthesis and characterization of a novel eco-friendly corrosion inhibition for mild steel in 1 M hydrochloric acid," Scientific reports, vol. 6, no. 19890, January 2016.

[15] Landolt, Dieter. (2007). *Corrosion and Surface Chemistry of Metals*. Swiss: EPFL Press.

[16] M. El Azhar, B. Mernari, M. Traisnel, F. Bentitss, and M. Lagrenee, "Corrosion inhibition of mild steel by the new class of inhibitors [2,5-bis(*n*-pyridyl)-1,3,4-thiadiazoles] in acidic media," J. Corros. Sci., vol. 43, pp. 2229-2238, December 2001.

[17] F. Bentiss., M. Lebrini., and M. Lagrenée. "Thermodynamic characterization of metal dissolution and inhibitor adsorption processes in mild steel/2,5-bis(n-thienyl)-1,3,4-thiadiazoles/ hydrochloricacid system," Corrosion Science vol. 47, pp. 2915–2931, December 2005.

[18] Luo, X., Pan, X., Yuan, S., Du, S., Zhang, C., and Liu, Y., "Corrosion inhibition of mild steel in simulated seawater solution by a green eco-friendly mixture of glucomannan (GL) and bisquaternary ammonium salt (BQAS)," Corrosion Science, vol. 125, pp. 139–151, June 2017.